
Tracking the Feature Dynamics in LLM Training: A Mechanistic Study

Yang Xu¹ Yi Wang¹ Hao Wang^{1†}

Abstract

Understanding training dynamics and feature evolution is crucial for the mechanistic interpretability of large language models (LLMs). Although sparse autoencoders (SAEs) have been used to identify features within LLMs, a clear picture of how these features evolve during training remains elusive. In this study, we: (1) introduce SAE-Track, a method to efficiently obtain a continual series of SAEs; (2) formulate the process of feature formation and conduct a mechanistic analysis; and (3) analyze and visualize feature drift during training. Our work provides new insights into the dynamics of features in LLMs, enhancing our understanding of training mechanisms and feature evolution.

Despite these advancements, the evolution of features during the training process—especially during pre-training—remains poorly understood. This knowledge gap is significant, as it hinders the ability to uncover how features emerge, stabilize, and transform over time. A deeper understanding of these dynamics would illuminate the mechanisms underpinning LLM training and offer valuable insights into their internal representations.

In this paper, we address this gap by conducting a comprehensive mechanistic analysis of feature evolution during the training of LLMs. Specifically, we study how features develop and stabilize in semantic meaning, and how they undergo directional changes. By doing so, we uncover novel insights into the dynamics of representation in LLMs.

Our contributions are summarized as follows:

1. Introduction

As LLMs increase in size and complexity, understanding their internal mechanisms has become a critical challenge. The emerging field of *mechanistic interpretability* seeks to decompose these models into interpretable components—such as induction heads (Olsson et al., 2022) and circuits (Conmy et al., 2023)—to analyze how these components interact and collectively drive model behavior. This approach represents a bottom-up pathway to demystify model representations.

A prominent direction within this field involves addressing *polysemanticity* in LLMs using Sparse Autoencoders (SAEs) (Bricken et al., 2023; Templeton et al., 2024). SAEs have been proposed as a technique for disentangling complex representations in LLMs by isolating features that are more interpretable and aligned with distinct semantic dimensions. Previous research has explored how these features vary across layers (Jack Lindsey et al., 2024; Balagansky et al., 2024), during fine-tuning stages (Jack Lindsey et al., 2024; Connor Kissane et al., 2024; Taras Kutsyk, 2024), and even between different models (Lan et al., 2024).

- **SAE-Track:** We introduce an efficient method for tracking feature evolution in LLMs through a continual SAE sequence across training checkpoints. SAE-Track enables detailed and reliable analysis of feature dynamics (Sec. 3).
- **Feature Evolution Phases and Patterns:** Using SAE-Track, we identify three distinct phases of feature evolution—*Initialization & Warmup*, *Emergent*, and *Convergent*—as well as three primary transformation patterns: *Maintaining*, *Shifting*, and *Grouping* (Sec. 4).
- **Formalization of Feature Formation:** We rigorously define the process of feature formation, which involves tracing the progression of features from noisy, unstructured activations to semantically meaningful representations. This includes examining how feature regions emerge and gain semantic fidelity (Sec. 5).
- **Analysis of Feature Drift:** We analyze feature drift, focusing on the directional evolution and trajectories of features. For a specific feature, its direction is the normalized decoder vector, while its trajectory is the decoder vector across training checkpoints, both of which capture the geometric evolution of features. Our study reveals that feature initially exhibit significant drift, continue to drift even after features are considered “formed,” and ultimately stabilize to their final state (Sec. 6).

[†]Corresponding author ¹Department of Computer Science, Rutgers University, New Jersey, USA. Correspondence to: Hao Wang <hw488@cs.rutgers.edu>.

- **Experiments Across Scales:** We validate our findings using LLM checkpoints of varying scales, demonstrating the generality and scalability of our approach.

2. Related Work

Sparse Autoencoders for Interpreting LLMs. A major challenge in interpreting LLMs is their polysemanticity, where individual neurons respond to mixtures of seemingly unrelated inputs. Based on the linear representation hypothesis (Park et al., 2023), research (Elhage et al., 2022) demonstrates that models can represent more features than their dimensionality allows, a phenomenon referred to as superposition, which might be a potential cause for polysemanticity. Sparse Autoencoders (SAEs), a dictionary learning method, address this issue by decoding the overlapping features in the space of model activation. Studies (Bricken et al., 2023; Cunningham et al., 2023) have used SAEs to uncover monosemantic features, while (Templeton et al., 2024) scaled this approach to identify features in the Claude 3 Sonnet.

SAEs have opened new pathways for investigating the relationship between feature geometry and semantic structure. For example, (Engels et al., 2024) extended the application of SAEs from one-dimensional to multi-dimensional representations, revealing irreducible multi-dimensional features. Furthermore, (Li et al., 2024) analyzed the geometry of features across scales, uncovering hierarchical patterns that reflect the organization of semantic representations within models. These studies highlight how SAEs can serve as tools for examining the geometric arrangement of model features.

While many representation studies focus on a single model at a fixed state, recent work has compared features across different states—such as layers (Jack Lindsey et al., 2024; Balagansky et al., 2024), between base and fine-tuned models (Jack Lindsey et al., 2024; Connor Kissane et al., 2024; Taras Kutsyk, 2024), and across different models entirely (Lan et al., 2024). However, the evolution of feature semantics and geometry *during training* (e.g., across different checkpoints/epochs) remains poorly understood. Our work addresses this gap by systematically analyzing feature evolution throughout training, revealing how feature representations develop and refine across checkpoints.

Mechanistic Study of Training Dynamics. Mechanistic studies on training dynamics have extensively explored the emergence of abilities in models. One notable example is grokking, a phenomenon in which models trained on small algorithmic tasks transition abruptly from overfitting to generalization after prolonged training (Power et al., 2022). This was further analyzed by (Nanda et al., 2023), which reverse-engineered the learning process and proposed

a method to measure the grokking progress. In a related vein, (Olsson et al., 2022) investigated the emerging in-context learning ability in LLMs, attributing this ability to the development of induction heads.

Other studies have investigated various facets of training dynamics. For instance, (Li et al., 2023) examined the training dynamics of transformers, focusing on how they develop topic structures during learning. They demonstrated that transformers encode topic structures by assigning higher average inner product values to embeddings of same-topic words and higher average pairwise attention between same-topic words. Additionally, (Qian et al., 2024) explored the trustworthiness of LLMs during pre-training, identifying distinct “fitting” and “compression” phases in the development of trustworthiness and introducing “steering vectors” as a method to enhance model alignment.

In contrast, our study is the first to use SAEs for a detailed investigation of the training dynamics of LLMs. By addressing polysemanticity and disentangling overlapping features, this approach reveals the dynamics of feature evolution during training and offers a new perspective for understanding model behavior.

3. SAE-Track: Getting a Continual Series of SAEs

3.1. Preliminaries: Sparse Autoencoders

In our setting, we primarily follow the formulation outlined in (Bricken et al., 2023; Templeton et al., 2024).

Let \mathbb{R}^D represent the activation space, where $\mathbf{x} \in \mathbb{R}^D$ denotes the residual stream activations in an LLM. We decompose this activation space into \mathbb{R}^F , where F corresponds to the dictionary size of the sparse autoencoder.

The basic structure of the Sparse Autoencoder (SAE) is given by:

$$\hat{\mathbf{x}} = \mathbf{b}^{\text{dec}} + \sum_{i=1}^F f_i(\mathbf{x}) \mathbf{W}_{:,i}^{\text{dec}}, \quad (1)$$

where $\mathbf{W}^{\text{dec}} \in \mathbb{R}^{D \times F}$ are the learned decoder weights, $\mathbf{b}^{\text{dec}} \in \mathbb{R}^D$ are the learned biases, and $f_i(\cdot)$ denotes the activation of encoded feature i . These feature activations are produced by the encoder using the following equation:

$$f_i(\mathbf{x}) = \text{ReLU}(\mathbf{W}_{i,:}^{\text{enc}} \cdot (\mathbf{x} - c \cdot \mathbf{b}^{\text{dec}}) + b_i^{\text{enc}}), \quad (2)$$

where $\mathbf{W}^{\text{enc}} \in \mathbb{R}^{F \times D}$ are the learned encoder weights, $\mathbf{b}^{\text{enc}} \in \mathbb{R}^F$ are the learned biases, and $c \in \{0, 1\}$ is a constant determining whether the decoder bias is included in the input transformation.

The loss function \mathcal{L} combines an ℓ_2 penalty on the recon-

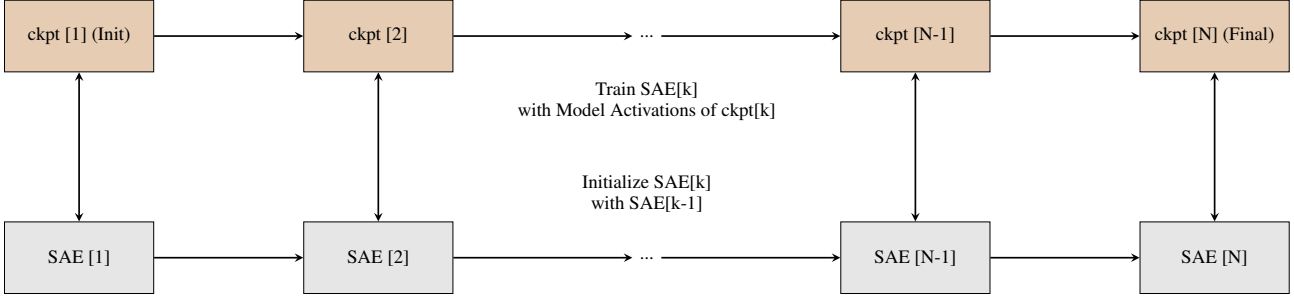


Figure 1. Illustration of the SAE-Track framework for tracking feature dynamics in LLMs. The top row represents training checkpoints (ckpt[k]) from initialization (ckpt[1]) to the final state (ckpt[N]). The bottom row shows Sparse Autoencoders (SAEs), each trained on activations from its corresponding checkpoint and initialized with parameters from the previous SAE (SAE[k - 1]). This design leverages a continual sequence of checkpoints, supporting efficient analysis of feature dynamics and real-time training as checkpoints become available sequentially.

struction error and an ℓ_1 penalty on the feature activations:

$$\mathcal{L} = \mathbb{E}_{\mathbf{x}} [\|\mathbf{x} - \hat{\mathbf{x}}\|_2^2 + \lambda \mathcal{L}_1], \quad (3)$$

where

$$\mathcal{L}_1 = \sum_i f_i(\mathbf{x}) \cdot \|\mathbf{W}_{:,i}^{\text{dec}}\|_2 \quad (4)$$

if there is no unit norm constraint on the decoder weights, or

$$\mathcal{L}_1 = \sum_i f_i(\mathbf{x}) \quad (5)$$

if the decoder weights have a unit norm constraint.

Several modifications have been proposed to improve SAE training, such as the TopK SAE (Gao et al., 2024) and JumpRELU SAE (Rajamanoharan et al., 2024). However, in this work, we use the standard SAE because its implementation is straightforward and it aligns with (Bricken et al., 2023; Templeton et al., 2024).

3.2. Intuitions and Our Method

To investigate the evolution of features in LLMs, Sparse Autoencoders (SAEs) must be trained on activations from each checkpoint. However, this process introduces several challenges:

1. **Stochasticity:** SAEs inherently encode features in a stochastic manner, meaning that each trained SAE may represent different features, even when derived from the same model. This variability introduces noise and makes feature analysis more challenging.
2. **Feature Alignment:** Aligning and comparing features across checkpoints is challenging due to potential inconsistencies in feature representations.

3. **Computational Overhead:** Training SAEs from scratch for all checkpoints is computationally expensive. For example, training SAEs across 154 checkpoints of the Pythia model would incur significant resource costs.

Thus, a more efficient and continual method is required to train SAEs across checkpoints. Before introducing our approach, we outline the guiding intuitions that informed its design.

3.2.1. INTUITIONS AND THEORY

SAEs are trained on activations that evolve incrementally during gradient descent. Leveraging the continuity of activation dynamics facilitates the efficient extraction of features and reduces noise when analyzing their evolution across checkpoints.

Formally, to analyze activation evolution in LLMs, we define the relationship between model parameters and activations. Let F denote the transformer model parameterized by Θ . Tokenized contexts $\{\mathcal{C}\}$ are used to train F , with Θ optimized via gradient descent to minimize the loss function \mathcal{L} .

We define $F^{(l,t)}$, where l denotes the transformer layer, t the training step, and $\Theta^{(<l,t)}$ the corresponding parameters. The activation for token q in context \mathcal{C} at layer l is:

$$\mathbf{x}^{(l,\mathcal{C},q,t)} = F^{(l,t)}(\mathcal{C}, q; \Theta^{(<l,t)}). \quad (6)$$

To simplify notation, we omit some components of the script (l, \mathcal{C}, q, t) in subsequent discussions for clarity.

Theorem 3.1 (Training-Step Continuity). Assume the following two conditions hold for all (\mathcal{C}, q) pairs: (1) **Gradient Bound:** The gradient norm $\|\nabla_{\Theta^{(<l,t)}} \mathcal{L}(\Theta)\| \leq G$ is bounded. (2) **Lipschitz Continuity:** The function $F^{(l)}$ is Lipschitz continuous with respect to parameters $\Theta^{(<l)}$, with a constant L .

If the learning rate satisfies $\eta < \frac{\epsilon}{LG}$, the activations evolve incrementally:

$$\left\| \mathbf{x}^{(l,t)} - \mathbf{x}^{(l,t-1)} \right\| < \epsilon. \quad (7)$$

The detailed proof is provided in Appendix B.

While real-world checkpoints do not guarantee a sufficiently small learning rate, leveraging the continuity of activation dynamics enables more efficient training and facilitates a continual series of SAEs to track the LLM.

3.2.2. OUR METHOD: RECURRENT INITIALIZATION AND TRAINING

Framework Overview. To track feature evolution, we train SAEs for a sequence of checkpoints $\text{ckpt}[1], \text{ckpt}[2], \dots, \text{ckpt}[N]$. As illustrated in Fig. 1, for each checkpoint $\text{ckpt}[k]$:

- SAE $[k]$ is initialized with parameters from SAE $[k-1]$ (with SAE $[1]$ initialized randomly), ensuring smooth transitions and reducing computational costs.
- SAE $[k]$ is trained on activations from checkpoint k .

Advantages. Our method has the following advantages:

- **Efficiency:** Incremental initialization significantly reduces training time; subsequent SAEs require approximately 1/20 of the initial training steps.
- **Continual Series of SAEs:** The method constructs a continual series of SAEs across checkpoints, providing a structured representation of feature evolution.
- **Real-Time Training:** The framework supports real-time training, allowing SAEs to be trained sequentially as checkpoints become available, without requiring access to all checkpoints upfront.

Experimental Setup. To prepare for subsequent studies, we trained SAEs on the residual stream before specific transformer layers. The experiments and analyses presented in the main paper are based on **Pythia-410m-deduped, layer=4**, while additional validations on **Pythia-160m-deduped, layer=4** and **Pythia-1.4b-deduped, layer=3** are detailed in Appendix C.3.

4. Overview: Feature Phases and Patterns

In this section, we provide an overview of how features evolve using our SAE-Track. By systematically analyzing feature development, we identify distinct patterns in their transformation across different phases of training.

Features extracted via SAEs are categorized into two types based on their activation behavior: **token-level features** and **concept-level features**. These categories highlight different roles and behaviors during training.

Definition 4.1 (Token-Level Feature). A *token-level feature* is a feature that predominantly activates for a specific token, such as “century.” These features can be identified early in training and generally exhibit a strong semantic association with individual tokens throughout the training process.

Definition 4.2 (Concept-Level Feature). A *concept-level feature* is a feature that activates across a set of tokens related to a concept with broader semantics. For example, tokens like “authentication” and “getRole()” can activate under a feature representing the concept “user authentication.” These features gradually develop semantic meaning as training progresses.

Token-level features typically exhibit semantic associations at every checkpoint, whereas concept-level features are initially noisy and lack meaningful structure. Over time, concept-level features gradually develop semantic coherence and align with broader abstract concepts. It is important to note that this is a general trend, as not all token-level features remain consistently associated with the same token throughout training.

We discuss the distinct phases of feature evolution in Sec. 4.1 and the specific transformation patterns for individual features in Sec. 4.2.

4.1. Phases of Feature Evolution

We find that the evolution of features can be divided into three distinct phases during training:

- **Initialization and Warmup.** Token-level features emerge at the very beginning of training, consistently activating for specific tokens. However, during this phase, features lack meaningful associations beyond individual tokens.
- **Emergent Phase.** Concept-level features begin to develop during this phase. Initially noisy, these features gradually align with abstract concepts, reflecting the model’s growing semantic understanding. Meanwhile, token-level features maintain their overall semantic associations.
- **Convergent Phase.** In the final training phase, both token-level and concept-level features converge to interpretable states. Concept-level features exhibit clear and coherent associations with semantic groups of tokens, indicative of the model’s matured representations.

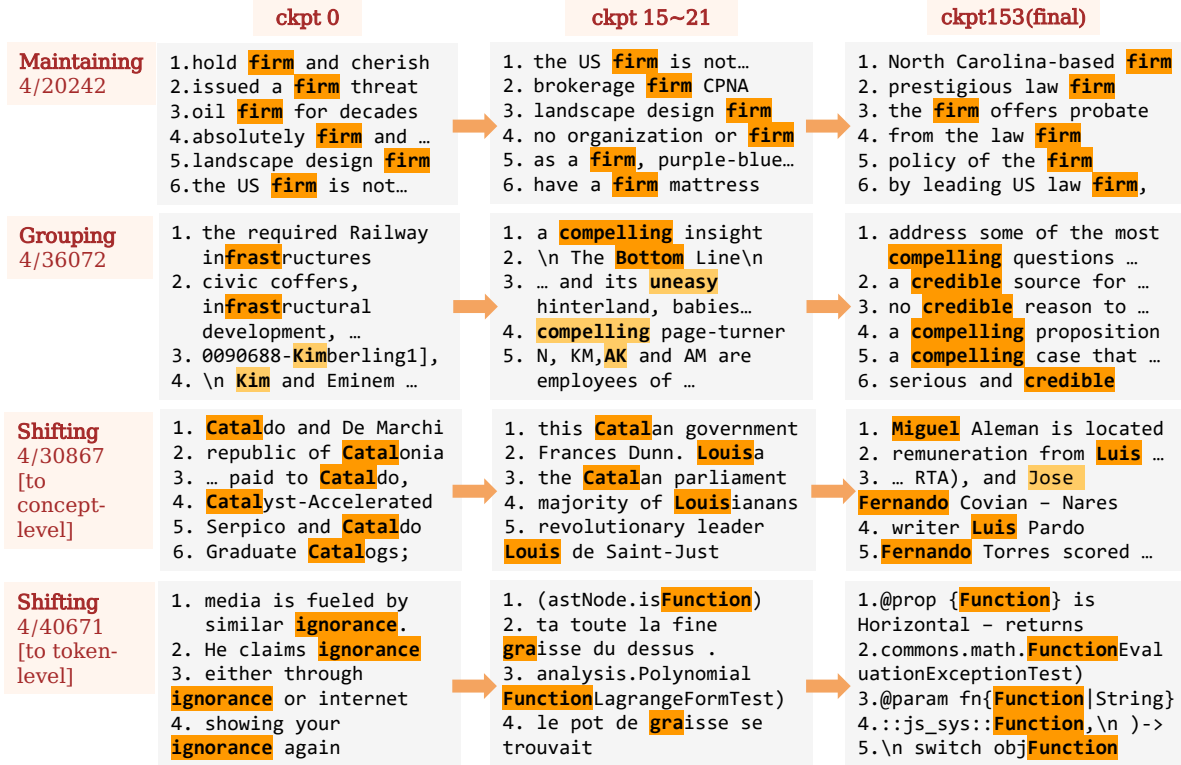


Figure 2. **Feature Evolution Patterns.** Illustration of the three primary feature evolution patterns during training: **Maintaining**, where features consistently activate for specific tokens across checkpoints; **Grouping**, where noisy features consolidate into cohesive and interpretable representations; and **Shifting**, where token-level features either transition to another token-level feature or evolve into concept-level features. Since concept-level features do not exist at initialization, **Shifting** exclusively begins from token-level features. The notation “layer/feature index” refers to the layer (preceding the residual stream) and the specific feature highlighted in the examples.

4.2. Patterns in Feature Transformation

We observe that feature evolution captured by SAE-Track can be characterized by three primary patterns:

- **Maintaining.** Some token-level features persist across training checkpoints, maintaining consistent activations for the same token. These features demonstrate minimal changes, highlighting their stability throughout training.
- **Shifting.** Certain token-level features transform, either aligning with a new token or evolving into concept-level features. This indicates a dynamic reorganization of feature associations during training.
- **Grouping.** Noisy features consolidate into cohesive and meaningful representations, forming distinct token-level or concept-level features. This grouping process reflects the model’s transition toward organized and interpretable features.

These patterns, as shown in Fig. 2, represent key phenomena

in feature evolution during training. **Maintaining** highlights the stability of certain token-level features across checkpoints. **Shifting** captures the dynamic transitions of features, either re-aligning with different tokens or evolving into concept-level features. **Grouping** reflects the consolidation of initially noisy features into coherent and interpretable structures. Collectively, these phenomena illustrate the progression from early-stage randomness to well-organized and semantically meaningful representations.

This section provides a high-level overview of the phases and patterns in feature evolution. Building on this foundation, the SAE series captured by SAE-Track enables a deeper exploration of two critical questions: how features form and whether feature directions drift during training or stabilize early on. These questions are examined in detail in Sec. 5 and Sec. 6.

5. Analysis of Feature Formation

In this section, we analyze how features transition from noisy activations to meaningful representations throughout

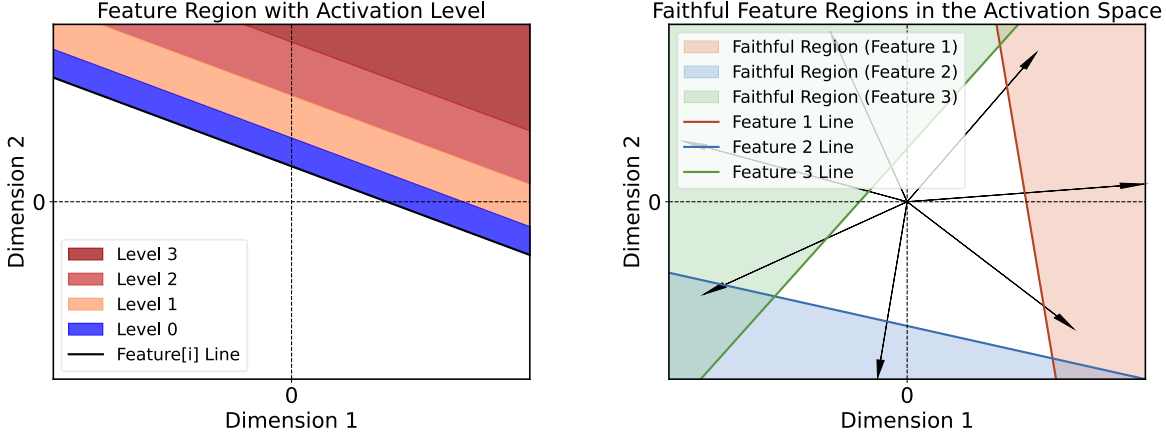


Figure 3. **Left:** A toy example illustrating feature regions with different activation levels in a 2D activation space. The colored regions represent varying activation intensities for a single feature, emphasizing the distinction between activation levels. **Right:** Faithful feature regions for three features, visualizing how features partition the activation space into semantically meaningful regions. This highlights the role of Sparse Autoencoder in isolating and identifying these regions.

training. We formally define key concepts, track the evolution of feature regions, and propose a Progress Measure to quantitatively assess this process in both activation and feature spaces.

5.1. What is Feature Formation?

Feature formation refers to the process by which a feature transitions from noise to a meaningful representation, ultimately gaining semanticity. Before formally defining feature formation, we address a fundamental question: **What is a feature across training checkpoints?**

What is a feature across checkpoints? Existing studies often emphasize the final state of training or assume that features are inherently monosemantic (Bricken et al., 2023; Templeton et al., 2024; Elhage et al., 2022). However, training a Sparse Autoencoder (SAE) at any model checkpoint—whether during random initialization, warm-up, emergence, or convergence—yields features that define separable regions in the activation space. While the specific properties of these features may vary across checkpoints, their presence highlights the dynamic and evolving nature of features throughout training.

Intuitively, a feature can be understood as a localized region in the activation space that activates under specific conditions. These regions naturally exist in the activation space, regardless of the model’s training phase. The role of the SAE is to identify and isolate these regions, providing a detailed understanding of feature representations and dynamics. Formally, the encoder for feature i can be expressed as:

$$f_i(\mathbf{x}) = \text{ReLU}\left(\widehat{\mathbf{W}}_i \cdot \mathbf{x} + \widehat{b}_i\right), \quad (8)$$

where $\widehat{\mathbf{W}}_i = \mathbf{W}_{i,:}^{\text{enc}}$ and $\widehat{b}_i = b_i^{\text{enc}} - c \cdot \mathbf{W}_{i,:}^{\text{enc}} \cdot \mathbf{b}^{\text{dec}}$. Using this, we define the “feature region” for feature i as follows:

Definition 5.1 (Feature Region). A region in the activation space that activates under feature i is defined as:

$$\mathcal{R}_i = \{\mathbf{x} \mid (\widehat{\mathbf{W}}_i \cdot \mathbf{x} + \widehat{b}_i) > 0\}, \quad (9)$$

where \mathbf{x} denotes the activation vector in LLMs.

While activation alone defines a feature region, it does not account for varying activation levels, which are critical for semantic fidelity. As noted by (Bricken et al., 2023), higher activation levels often correspond to stronger associations with specific tokens or concepts, reflecting the semantic significance of features. In Fig. 3 (left), a 2D toy example illustrates how varying activation levels delineate distinct regions. Building on this, we refine the definition to incorporate activation levels as follows:

Definition 5.2 (Feature Region with Activation Level). A region corresponding to feature i with activation level $[L, U)$ is defined as:

$$\mathcal{R}_i^{[L,U)} = \{\mathbf{x} \mid L \leq (\widehat{\mathbf{W}}_i \cdot \mathbf{x} + \widehat{b}_i) < U\}. \quad (10)$$

To assess semantic fidelity, we assume a threshold L_i beyond which a feature is considered semantically meaningful. This is formalized as:

Definition 5.3 (Faithful Feature Region). A region that faithfully represents feature i is defined as:

$$\mathcal{R}_i^{\text{faithful}} = \mathcal{R}_i^{[L_i, \infty)}, \quad (11)$$

where L_i is the threshold activation level required for semantic fidelity.

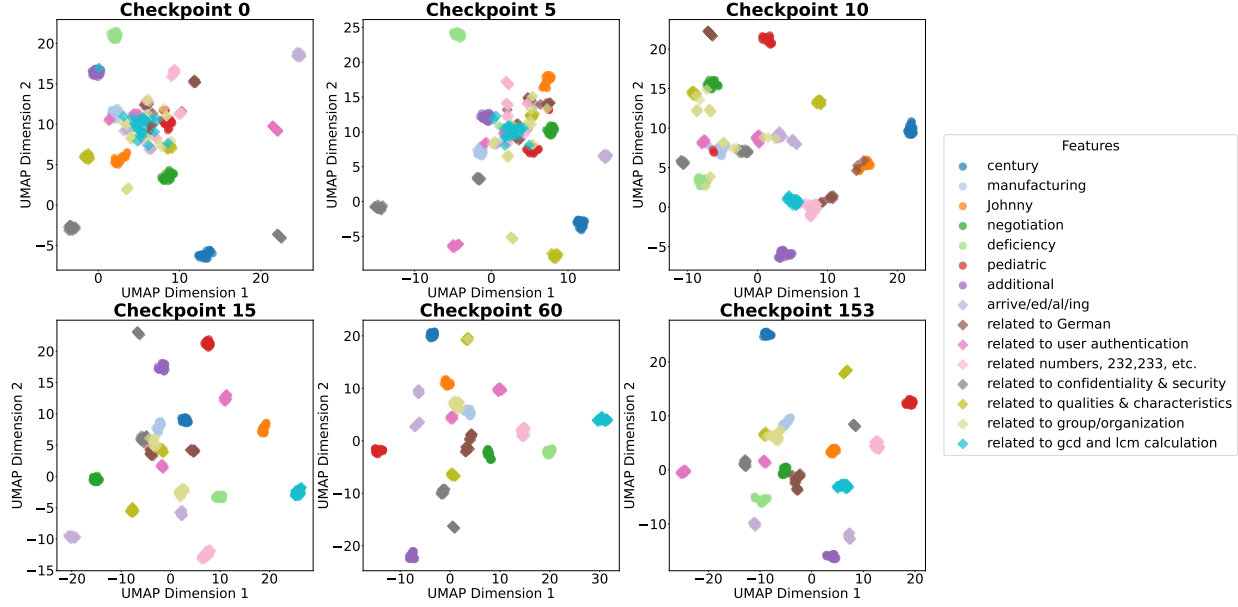


Figure 4. UMAP Visualization. UMAP illustrates the evolution of activation sets for various features across training checkpoints, with each colored point representing a datapoint associated with a distinct feature. Circular markers indicate token-level features, while diamond-shaped markers represent concept-level features. The visualization highlights the transition from random activations at the start of training (Checkpoint 0) to semantically coherent clusters at later stages (Checkpoint 153) and showcases the distinct dynamics of the two feature types.

In Fig. 3 (right), a toy example demonstrates how the faithful regions of three features partition a 2D activation space. This example highlights the SAE’s objective to identify these regions and provides insights into the geometric structure of the activation space.

Feature formation describes how datapoints with similar semantics converge into faithful feature regions in the activation space. To study this phenomenon, we track the evolution of datapoints within the same faithful feature region. Using the SAE at the final checkpoint, we define $\{\mathcal{R}_i^{\text{faithful}}[t = T_{\text{final}}]\}_{i=0}^{F-1}$ as the ground truth. Let \mathcal{D}_i denote the set of datapoints that activate within $\mathcal{R}_i^{\text{faithful}}[T_{\text{final}}]$ at the final checkpoint, i.e.,

$$\mathcal{D}_i = \{(\mathcal{C}, q) \mid F^{(T_{\text{final}})}(\mathcal{C}, q; \Theta^{(T_{\text{final}})}) \in \mathcal{R}_i^{\text{faithful}}[T_{\text{final}}]\}, \quad (12)$$

where \mathcal{C} represents the context and q denotes the token position within \mathcal{C} . The activation set of these datapoints at training step t is defined as:

$$\mathcal{A}_i^t = \{F^{(t)}(\mathcal{C}, q; \Theta^{(t)}) \mid (\mathcal{C}, q) \in \mathcal{D}_i\}. \quad (13)$$

Here, \mathcal{A}_i^t represents the activations at checkpoint t for all datapoints in \mathcal{D}_i . Thus, studying feature formation involves analyzing the dynamics of $\{\mathcal{A}_i^t\}_{i=0}^{F-1}$ across training.

5.2. Visualization and Analysis

By tracking $\{\mathcal{A}_i^t\}_{i=0}^{F-1}$ across training steps t , we visualize the process of feature formation. Using UMAP (McInnes et al., 2020), we project the activation sets of various features across checkpoints (see Fig. 4, more detailed below). Datapoints with the top 25 feature activations are considered faithful, highlighting the dynamics of both token-level and concept-level features.

Initialization and Warmup Phase: Token-level feature datapoints form distinct clusters, while concept-level feature datapoints remain scattered.

In Fig. 4, Checkpoint 0, the initialized network demonstrates tightly clustered datapoints for token-level features. These datapoints (\mathcal{C}, q) correspond to identical tokens with highly similar contexts \mathcal{C} . When the input is passed through a transformer F with randomized parameters Θ_{rand} , the resulting activations exhibit high similarity, primarily determined by the shared token and its repetitive context. In contrast, concept-level features remain scattered, as they require the model to abstract and generalize across related tokens—a capability that does not emerge from a randomized transformer. This phase represents the early state of feature development, where only basic token-level associations are evident.

Emergent Phase: Concept-level features begin to form.

As training progresses (Fig. 4, Checkpoints 5, 10, and 15), concept-level features gradually evolve from noisy, scat-

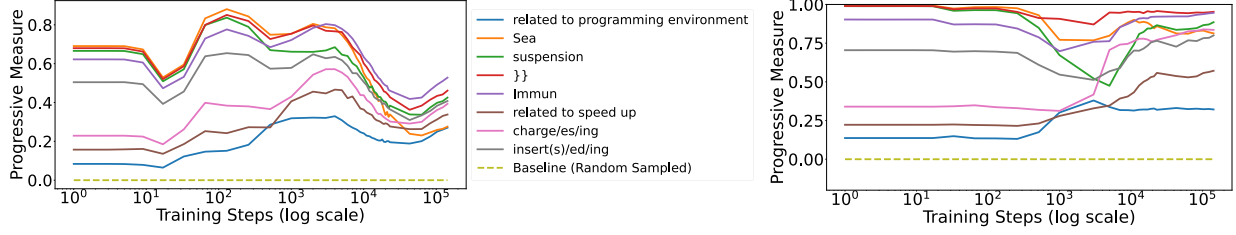


Figure 5. **Left:** Progress Measure in the activation space across training steps (log scale) for various features. **Right:** Progress Measure in the feature space across training steps (log scale) for the same features. Both plots illustrate the distinct dynamics of different types of features during training.

tered points into more cohesive clusters. This transition reflects the model’s growing capacity to capture semantic abstractions and represent higher-order concepts. Meanwhile, token-level features remain tightly clustered and stable throughout this phase.

Convergent Phase: All features reach a stable and fully formed state. By Fig. 4, Checkpoints 60 and 153, both token-level and concept-level features have reached a stable and well-formed state. Datapoints of all features are tightly clustered, reflecting the model’s fully developed ability to represent both specific tokens and broader semantic concepts with high fidelity.

These visualizations at Fig. 4 across various checkpoints vividly illustrate the evolution of features, highlighting their transition from early random activations to semantically meaningful and well-defined clusters.

5.3. Progress Measure

Is feature formation a phase transition or a progressive process? To answer this question, we propose the **Feature Formation Progress Measure**, which quantifies the degree to which a feature becomes well-formed during training. This measure compares the similarity within semantic datapoints to a baseline derived from randomly sampled, unrelated datapoints.

Definition 5.4 (Feature Formation Progress Measure). The metric $M_i(t)$ at training step t is defined as:

$$M_i(t) = \overline{Sim}_{\mathcal{A}_i^t} - \overline{Sim}_{\mathcal{A}_{random}}, \quad (14)$$

where \mathcal{A}_{random} represents a set of randomly sampled datapoints, and:

$$\overline{Sim}_{\mathcal{A}_i^t} = \frac{2}{|\mathcal{A}_i^t|(|\mathcal{A}_i^t|-1)} \sum_{\substack{x_k, x_j \in \mathcal{A}_i^t \\ j < k}} Sim(x_k, x_j), \quad (15)$$

$$\overline{Sim}_{\mathcal{A}_{random}} = \frac{2}{|\mathcal{A}_{random}|(|\mathcal{A}_{random}|-1)} \sum_{\substack{x_k, x_j \in \mathcal{A}_{random} \\ j < k}} Sim(x_k, x_j). \quad (16)$$

To extend the analysis to feature space, we define a corresponding measure:

$$M_i^{feature}(t) = \overline{Sim}_{\mathcal{F}_i^t} - \overline{Sim}_{\mathcal{F}_{random}}, \quad (17)$$

where:

$$\overline{Sim}_{\mathcal{F}_i^t} = \frac{2}{|\mathcal{F}_i^t|(|\mathcal{F}_i^t|-1)} \sum_{\substack{f_k, f_j \in \mathcal{F}_i^t \\ j < k}} Sim(f_k, f_j), \quad (18)$$

$$\overline{Sim}_{\mathcal{F}_{random}} = \frac{2}{|\mathcal{F}_{random}|(|\mathcal{F}_{random}|-1)} \sum_{\substack{f_k, f_j \in \mathcal{F}_{random} \\ j < k}} Sim(f_k, f_j). \quad (19)$$

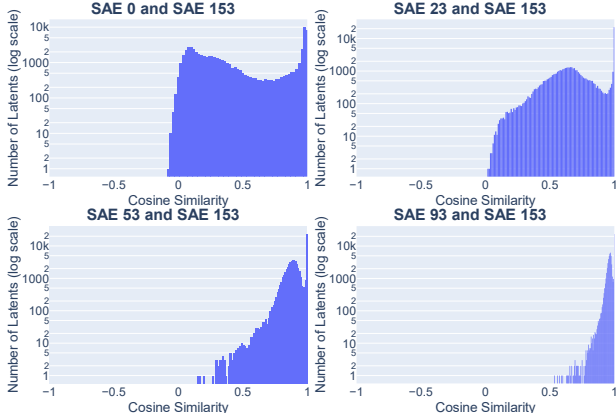
Here, \mathcal{F}_i^t represents the feature set of datapoints encoded by the SAE encoder at training step t , while \mathcal{F}_{random} denotes the feature set for randomly sampled datapoints encoded in the same manner. By incorporating the feature space, this measure provides a finer-grained perspective on how datapoints align with features, offering valuable insights into the process of feature formation.

$Sim(\cdot, \cdot)$ can be computed using various metrics, such as cosine similarity or Jaccard similarity. In Fig. 5 (**Left** for activation space and **Right** for feature space), we employ cosine similarity to demonstrate the utility of the proposed Progress Measure in capturing the gradual formation of features. Experiments with alternative similarity measures (e.g., Jaccard similarity) yield consistent results, as detailed in Appendix C.2, validating the robustness of this metric.

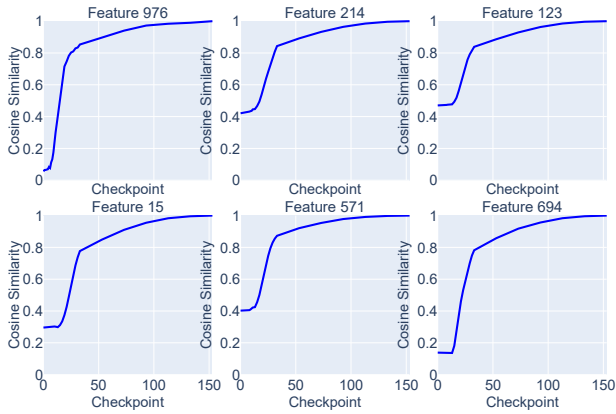
Notably, our Progress Measure highlights the dynamic evolution of token-level and concept-level features, providing a quantitative perspective on feature formation. This complements the qualitative insights presented in Sec. 5.2.

6. Analysis of Feature Drift

Do feature directions drift during training, or do they stabilize early on? **Our study reveals that feature directions initially exhibit significant drift, continue to shift even after features are considered “formed,” and ultimately**



(a) Distribution of cosine similarity between decoder vectors at intermediate training checkpoints and the final checkpoint.



(b) Cosine similarity progression for sampled features across training checkpoints. Each subplot traces how individual features progressively approach their final direction.

Figure 6. Decoder Vector Evolution. Distribution and progression of cosine similarity between decoder vectors at intermediate checkpoints and their final state, illustrating both global alignment trends and individual feature dynamics throughout training.

stabilize to their final state. A feature is considered *formed* once it gains semantic meaning, which typically stabilizes its semantic association. However, our analysis shows that directional drift persists during training, reflecting ongoing refinements in the feature geometry before reaching stability.

6.1. Decoder Vector Evolution

Our analysis examines the evolution of decoder vectors $\{\mathbf{W}_{:,i}^{\text{dec}}\}_{i=0}^{F-1}$, which represent an overcomplete basis for the activation space. These vectors define the geometric representation of each feature and its contribution to reconstructing the activations. Following (Templeton et al., 2024), the direction of a feature i is defined as $\frac{\mathbf{W}_{:,i}^{\text{dec}}}{\|\mathbf{W}_{:,i}^{\text{dec}}\|}$.

To study the evolution of feature directions, we calculate the cosine similarity between decoder vectors at different training checkpoints. This quantifies how closely the directions of features at time t align with their final state at $t = \text{final}$.

Our analysis uses two complementary perspectives. Fig. 6(a) provides a checkpoint-centric view, summarizing the cosine similarity of all features at a given training time relative to their final state. This perspective offers a global snapshot of the model’s progress in refining feature directions, revealing that feature directions in LLMs do not remain static during training. Instead, most features exhibit significant drift and gradually align with their final state as training progresses.

In contrast, Fig. 6(b) adopts a feature-centric view, illustrating how the similarity of a specific feature with its final state evolves across all training checkpoints. This visualization shows that the similarity initially remains relatively stable, then experiences a sudden increase during training, and gradually transitions into a plateau as it approaches the end. These trends align with the three phases we previously identified: *Initialization & Warmup*, *Emergent*, and *Convergent*. Together, these two perspectives complement each other, providing consistent yet distinct insights into the directional changes of feature evolution during training.

6.2. Trajectory Analysis

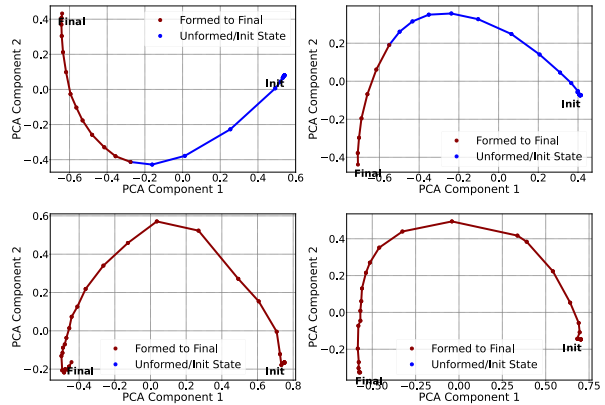


Figure 7. Feature Trajectories. Trajectories of decoder vectors represent the directional change of features across training checkpoints. “Dark red” indicates features that are considered “formed,” i.e., they have gained semantic meaning and generally remain stable semantic meaning until the final state. “Blue” indicates features that are still unformed or in the initial stage.

Building on the analysis of decoder vector evolution, we now examine feature trajectories to gain a deeper understanding of how features evolve across training checkpoints. By distinguishing the phases before and after a feature gains semantic meaning, we can better understand the relationship between directional drift and feature formation. This distinction highlights how drift persists even after feature

formation, providing insights into the continuous adjustments in the feature space throughout training.

Definition 6.1 (Feature Trajectory). Let $\mathbf{W}_{:,i}^{dec}[t]$ denote the decoder vector for feature i at training checkpoint t , where $t \in \{1, \dots, T_{final}\}$. The trajectory of feature i is defined as:

$$\mathcal{J}_i = \{\mathbf{W}_{:,i}^{dec}[1], \mathbf{W}_{:,i}^{dec}[2], \dots, \mathbf{W}_{:,i}^{dec}[T_{final}]\}. \quad (20)$$

A feature is considered formed once it gains and stabilizes in semantic meaning. This means that trajectories exhibiting (“maintaining”) behavior are always in the formed state, whereas those exhibiting (“shifting”) or (“grouping”) behaviors transition into the formed state later during training and remain in this state until the final checkpoint.

As shown in Fig. 7, feature trajectories transition from an unformed phase (blue) to a formed phase (dark red), with maintaining behaviors consistently in the formed state and shifting or grouping behaviors transitioning into it during training, illustrating the dynamic relationship between directional drift and feature formation.

7. Conclusion

In this paper, we conduct a comprehensive mechanistic analysis of feature evolution in LLMs during training: (1) We propose SAE-Track, a novel method for obtaining a continual series of Sparse Autoencoders (SAEs) across training checkpoints, enabling efficient and stable feature tracking. (2) We formalize the concept of feature formation, tracking the progression of features from noise to semantic fidelity. (3) We analyze feature drift, showing that feature directions initially exhibit significant adjustments and continue to shift even after features gain semantic meaning, before ultimately stabilizing at the final checkpoint. Our work provides a detailed understanding of how features evolve and stabilize during training, offering insights into the underlying mechanisms of feature formation and drift in LLMs.

References

- Balagansky, N., Maksimov, I., and Gavrillov, D. Mechanistic permutability: Match features across layers, 2024.
- Biderman, S., Schoelkopf, H., Anthony, Q. G., Bradley, H., O’Brien, K., Hallahan, E., Khan, M. A., Purohit, S., Prashanth, U. S., Raff, E., et al. Pythia: A suite for analyzing large language models across training and scaling. In *International Conference on Machine Learning*, pp. 2397–2430. PMLR, 2023.
- Bricken, T., Templeton, A., Batson, J., Chen, B., Jermyn, A., Conerly, T., Turner, N., Anil, C., Denison, C., Askell, A., et al. Towards monosemanticity: Decomposing language models with dictionary learning. *Transformer Circuits Thread*, 2, 2023.
- Chalnev, S., Siu, M., and Conmy, A. Improving steering vectors by targeting sparse autoencoder features, 2024.
- Conmy, A., Mavor-Parker, A., Lynch, A., Heimersheim, S., and Garriga-Alonso, A. Towards automated circuit discovery for mechanistic interpretability. *Advances in Neural Information Processing Systems*, 36:16318–16352, 2023.
- Connor Kissane, robertzk, Arthur Conmy, and Neel Nanda. Saes (usually) transfer between base and chat models, 2024.
- Cunningham, H., Ewart, A., Riggs, L., Huben, R., and Sharkey, L. Sparse autoencoders find highly interpretable features in language models, 2023.
- Elhage, N., Hume, T., Olsson, C., Schiefer, N., Henighan, T., Kravec, S., Hatfield-Dodds, Z., Lasenby, R., Drain, D., Chen, C., et al. Toy models of superposition. *arXiv preprint arXiv:2209.10652*, 2022.
- Engels, J., Liao, I., Michaud, E. J., Gurnee, W., and Tegmark, M. Not all language model features are linear. *arXiv preprint arXiv:2405.14860*, 2024.
- Farrell, E., Lau, Y.-T., and Conmy, A. Applying sparse autoencoders to unlearn knowledge in language models, 2024.
- Gao, L., Biderman, S., Black, S., Golding, L., Hoppe, T., Foster, C., Phang, J., He, H., Thite, A., Nabeshima, N., Presser, S., and Leahy, C. The Pile: An 800gb dataset of diverse text for language modeling. *arXiv preprint arXiv:2101.00027*, 2020.
- Gao, L., la Tour, T. D., Tillman, H., Goh, G., Troll, R., Radford, A., Sutskever, I., Leike, J., and Wu, J. Scaling and evaluating sparse autoencoders, 2024.
- hijohnnylin. mats_sae_training. <https://github.com/jbloomAus/SAELens>, 2024.
- Jack Lindsey, Adly Templeton, Jonathan Marcus, Thomas Conerly, Joshua Batson, and Christopher Olah. Sparse crosscoders for cross-layer features and model diffing. *Transformer Circuits Thread*, 2024.
- Joseph Bloom, C. T. and Chanin, D. Saelens. <https://github.com/jbloomAus/SAELens>, 2024.
- Lan, M., Torr, P., Meek, A., Khakzar, A., Krueger, D., and Barez, F. Sparse autoencoders reveal universal feature spaces across large language models, 2024.

- Li, Y., Li, Y., and Risteski, A. How do transformers learn topic structure: Towards a mechanistic understanding. In *International Conference on Machine Learning*, pp. 19689–19729. PMLR, 2023.
- Li, Y., Michaud, E. J., Baek, D. D., Engels, J., Sun, X., and Tegmark, M. The geometry of concepts: Sparse autoencoder feature structure, 2024.
- McDougall, C. SAE Visualizer. https://github.com/callumcdougall/sae_vis, 2024.
- McInnes, L., Healy, J., and Melville, J. Umap: Uniform manifold approximation and projection for dimension reduction, 2020.
- Nanda, N. and Bloom, J. Transformerlens. <https://github.com/TransformerLensOrg/TransformerLens>, 2022.
- Nanda, N., Chan, L., Lieberum, T., Smith, J., and Steinhart, J. Progress measures for grokking via mechanistic interpretability. *arXiv preprint arXiv:2301.05217*, 2023.
- Olsson, C., Elhage, N., Nanda, N., Joseph, N., DasSarma, N., Henighan, T., Mann, B., Askell, A., Bai, Y., Chen, A., et al. In-context learning and induction heads. *arXiv preprint arXiv:2209.11895*, 2022.
- Park, K., Choe, Y. J., and Veitch, V. The linear representation hypothesis and the geometry of large language models. *arXiv preprint arXiv:2311.03658*, 2023.
- Power, A., Burda, Y., Edwards, H., Babuschkin, I., and Misra, V. Grokking: Generalization beyond overfitting on small algorithmic datasets, 2022.
- Qian, C., Zhang, J., Yao, W., Liu, D., Yin, Z., Qiao, Y., Liu, Y., and Shao, J. Towards tracing trustworthiness dynamics: Revisiting pre-training period of large language models. *arXiv preprint arXiv:2402.19465*, 2024.
- Rajamanoharan, S., Lieberum, T., Sonnerat, N., Conmy, A., Varma, V., Kramár, J., and Nanda, N. Jumping ahead: Improving reconstruction fidelity with jumprelu sparse autoencoders, 2024.
- Taras Kutsyk, Tommaso Mencattini, C. F. Do sparse autoencoders (saes) transfer across base and finetuned language models?, 2024.
- Templeton, A., Conerly, T., Marcus, J., Lindsey, J., Bricken, T., Chen, B., Pearce, A., Citro, C., Ameisen, E., Jones, A., et al. Scaling monosemanticity: extracting interpretable features from claude 3 sonnet, transformer circuits thread, 2024.

A. Discussion

A.1. Dead Features and Ultra-Low Activation Features

In our analysis, we exclude two categories of features that fail to contribute meaningful information during training:

- **Dead Features:** These are features that remain inactive throughout the entire training process, i.e., they do not activate on any datapoint at any checkpoint. Such features are entirely uninformative and irrelevant to the study of feature formation.
- **Ultra-Low Activation Features:** Features with extremely low activation densities or values are also excluded. While not strictly inactive, these features exhibit negligible activations that render them semantically meaningless. This filtering is consistent with prior observations in (Bricken et al., 2023), which identify such low-activation features as non-contributive to representation learning.

By filtering these two types of features, we focus on those that exhibit meaningful activations and contribute to the evolving structure of the activation space, enabling a clearer study of feature dynamics.

A.2. Special Cases of Features

Weak Concept-Level Features. Concept-level features with limited variants, such as morphological features corresponding to suffixes (e.g., *-ed*, *-ing*), can be considered weak concept-level features. For instance, a feature might primarily activate for 10 occurrences of *-ing* and 15 of *-ed*, leading to repeated pairings during similarity calculations. This repetition often inflates similarity scores in similarity-based metrics, despite these features being fundamentally identical in nature to typical concept-level features.

At the start of training, datapoints corresponding to weak features often form multiple separate clusters in the activation space. However, this clustering is a superficial phenomenon that reflects redundancy rather than meaningful semantic coherence. Only via training does the model gradually learn to organize these datapoints into a single cohesive feature.

Polysemous Token-Level Features. For polysemous tokens—tokens with multiple meanings—the corresponding token-level features may initially activate without capturing any semantic distinctions. During the early training phase, these features are primarily activated based on token identity alone. However, as training progresses and the model learns to incorporate semantics, these features sometimes degrade to represent only the most prominent meaning of the token. This degradation reflects the model’s learning process, where it begins to understand and refine what a token-level feature truly represents, prioritizing the most frequent or contextually significant meaning.

A.3. The Challenge of Tracking Initial Features

One might expect that all features observed during the initialization stage can be consistently tracked throughout training. However, this is not feasible due to three key reasons:

- **Emergent Phase Dynamics:** During the emergent phase, activations corresponding to initially distinct datapoints may overlap or merge, resulting in features that no longer align with their initial definitions.
- **SAE Training Property:** SAE training can be viewed as selecting features from a large pool of possible features to explain the model activations (Templeton et al., 2024). Even when training SAEs twice on the same model activations and data, divergence in learned features can occur (Bricken et al., 2023). This selection process inherently introduces inconsistencies between initial and final features as the learned features adapt to the evolving data representations.
- **Shifting Phenomenon:** Unlike the initial checkpoint, where SAEs mainly produce token-level features, the final checkpoint SAEs are not constrained to token-level representations. As training progresses, features initially aligned to specific tokens may shift and evolve into other features. This transformation makes strict feature tracking across checkpoints impractical.

It is important to emphasize that SAE-Track is designed as a study tool rather than an engineering evaluation framework. The goal is to provide insights into feature dynamics, not to enforce strict feature-tracking consistency.

A.4. Implications and Practical Potential

- **Study’s Implications: Mechanistic Understanding of Training Dynamics.** Our study provides a systematic analysis of how features form and evolve progressively throughout training, offering deeper insights into the internal representations of LLMs. By examining feature dynamics across checkpoints, this work paves the way for future research to better understand the learning processes of different knowledge types and the emergence of higher-order semantics.
- **Practical Potential: Real-Time Intervention.** SAE-Track allows Sparse Autoencoders (SAEs) to be trained synchronously with LLMs at low cost, enabling real-time analysis of feature evolution during training. Since feature formation is a gradual and progressive process, this setup opens the possibility of early detection and intervention for unsafe or undesired features before they solidify. Prior works have attempted interventions using SAEs (Templeton et al., 2024; Farrell et al., 2024; Chalnev et al., 2024), and our method and study provides a promising future direction for improving model safety and alignment.

B. Detailed Derivation of the Training-Step Continuity Theorem

Assume the conditions hold. Using a first-order Taylor expansion:

$$\mathbf{x}^{(l,t)} \approx \mathbf{x}^{(l,t-1)} + \left. \frac{\partial F^{(l)}}{\partial \Theta^{(<l)}} \right|_{\Theta^{(<l,t-1)}} \cdot (\Theta^{(<l,t)} - \Theta^{(<l,t-1)}). \quad (21)$$

Substituting the gradient descent update $\Theta^{(<l,t)} - \Theta^{(<l,t-1)} = -\eta \nabla_{\Theta^{(<l)}} \mathcal{L}(\Theta^{(t-1)})$, we have:

$$\mathbf{x}^{(l,t)} \approx \mathbf{x}^{(l,t-1)} - \eta \left. \frac{\partial F^{(l)}}{\partial \Theta^{(<l)}} \right|_{\Theta^{(<l,t-1)}} \cdot \nabla_{\Theta^{(<l)}} \mathcal{L}(\Theta^{(t-1)}). \quad (22)$$

Taking norms and applying the bounds on $\frac{\partial F^{(l)}}{\partial \Theta^{(<l)}}$ and $\nabla_{\Theta^{(<l)}} \mathcal{L}(\Theta)$:

$$\left\| \mathbf{x}^{(l,t)} - \mathbf{x}^{(l,t-1)} \right\| \leq \eta LG. \quad (23)$$

With $\eta < \frac{\epsilon}{LG}$, this ensures:

$$\left\| \mathbf{x}^{(l,t)} - \mathbf{x}^{(l,t-1)} \right\| < \epsilon, \quad (24)$$

proving continuous activation changes over training steps.

This derivation supports the Training-Step Continuity Theorem by bounding activation changes through Lipschitz continuity and gradient norms. The result highlights the incremental and stable evolution of activations during training.

C. Experimental details and more results

C.1. Implementation Details

Most experiments were conducted on a single NVIDIA A100 GPU. The implementation is built primarily upon the frameworks and methodologies introduced in (McDougall, 2024; Joseph Bloom & Chanin, 2024; hijohnnylin, 2024; Nanda & Bloom, 2022).

Model: We use the Pythia-deduped models (Biderman et al., 2023) for our experiments, which provide 154 checkpoints across training. This deduplicated version ensures a cleaner training dataset, reducing noise and redundancy. The extensive set of checkpoints enables detailed tracking of feature evolution over time. The checkpoints are:

$$[0, 1, 2, 4, 8, 16, 32, 64, 128, 256, 512] + \text{list}(\text{range}(1000, 143000 + 1, 1000)). \quad (25)$$

We conduct experiments on three Pythia scales: 160M, 410M, and 1.4B parameters, ensuring consistency across different model sizes.

Dataset: The deduplicated version of the Pile dataset (Gao et al., 2020) is used, aligning with the Pythia-deduped models. This ensures minimal repetition in the training data, further improving the quality of feature extraction.

SAEs Training: To efficiently train Sparse Autoencoders (SAEs) across multiple checkpoints, we employ a recurrent initialization scheme, which reuses the weights from the previous checkpoint to initialize the current SAE. The checkpoints for SAE training are selected based on the following adaptive schedule:

$$\text{list}(\text{range}(12)) + \text{list}(\text{range}(13, 33, 2)) + \text{list}(\text{range}(33, 153, 20)). \tag{26}$$

This piecewise linear schedule adjusts the density of selected checkpoints across different training phases. For example, during the convergent phase, fewer checkpoints (e.g., 113, 133, 153) are sufficient, as feature evolution slows down. This strategy reduces computational costs while maintaining high representation quality.

Overtraining is applied to enhance feature representations, as recommended in (Bricken et al., 2023). By leveraging the recurrent initialization scheme, which reuses pretrained weights, convergence is significantly accelerated. Specifically, only about $\frac{1}{20}$ of the initial training tokens are required for subsequent SAEs, resulting in substantial computational savings.

C.2. Different Similarity Metrics

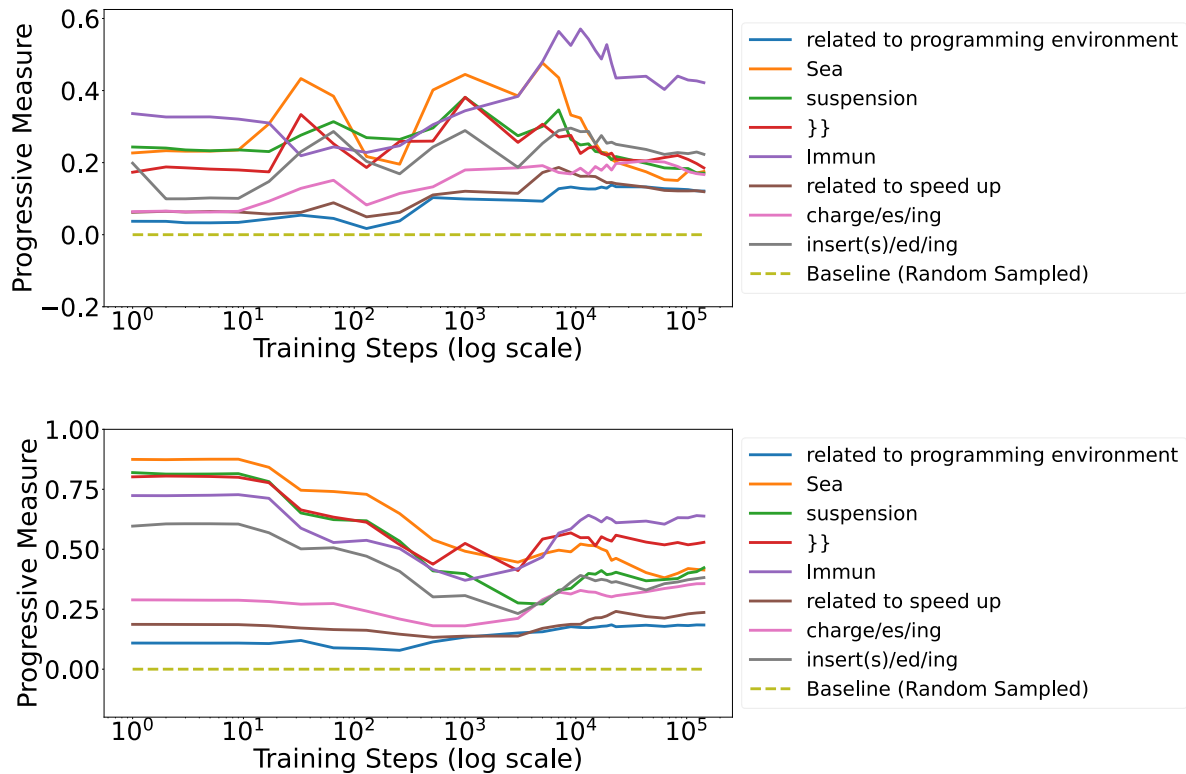


Figure 8. **Progress Measure using different similarity metrics.**Top: jaccard similarity for feature space, Bottom: weighted jaccard similarity for feature space

Our progress measure relies on the choice of similarity metrics. In the main text, we use cosine similarity; here, we extend the analysis by exploring additional metrics, as shown in Fig. 8. The results demonstrate that the overall trend remains consistent across different metrics. Specifically, token-level features exhibit relatively stable high values, while concept-level features gradually increase in similarity metric values as training progresses. Importantly, the choice of similarity metric does not significantly affect the overall analysis or conclusions.

Definitions of Similarity Metrics:

- **Cosine Similarity:** Cosine similarity, applied to the activation space with new datapoints, measures the angular

similarity between two vectors \mathbf{u} and \mathbf{v} . It is defined as:

$$\text{CosSim}(\mathbf{u}, \mathbf{v}) = \frac{\mathbf{u} \cdot \mathbf{v}}{\|\mathbf{u}\| \|\mathbf{v}\|}, \quad (27)$$

where $\mathbf{u} \cdot \mathbf{v}$ denotes the dot product, and $\|\mathbf{u}\|$, $\|\mathbf{v}\|$ are the norms of the respective vectors.

- **Jaccard Similarity:** Jaccard similarity is applied to the sparse feature space. It converts each feature vector into a binary representation, indicating whether a feature is activated (1) or not (0), and calculates similarity as:

$$\text{Jaccard}(\mathbf{u}, \mathbf{v}) = \frac{|\mathbf{u}_{\text{binary}} \cap \mathbf{v}_{\text{binary}}|}{|\mathbf{u}_{\text{binary}} \cup \mathbf{v}_{\text{binary}}|}, \quad (28)$$

where $\mathbf{u}_{\text{binary}}$ and $\mathbf{v}_{\text{binary}}$ are the binary representations of \mathbf{u} and \mathbf{v} , respectively.

- **Weighted Jaccard Similarity:** Weighted Jaccard similarity extends Jaccard similarity by considering the magnitude of activations in the feature space. For two activation vectors \mathbf{u} and \mathbf{v} , it is defined as:

$$\text{WeightedJaccard}(\mathbf{u}, \mathbf{v}) = \frac{\sum_i \min(u_i, v_i)}{\sum_i \max(u_i, v_i)}, \quad (29)$$

where u_i and v_i are the activation values for feature i in \mathbf{u} and \mathbf{v} , respectively.

Since Jaccard and Weighted Jaccard are more suitable for sparse vectors, and their meaning becomes less significant for non-sparse vectors, we restrict their use to the feature space. The overall trends presented in Fig. 8 demonstrate that the choice of metric does not substantially affect the study’s conclusions.

C.3. Experiments on Different Model Scales

Below, we present results for **Pythia-160m-deduped, layer=4** and **Pythia-1.4b-deduped, layer=3**, trained on the residual stream before the specified layers. The figures include UMAP projections, progress measures, decoder cosine similarity, and trajectory analysis. These results align closely with those observed for **Pythia-410m-deduped, layer=4** in the main paper, highlighting the consistency of our results.

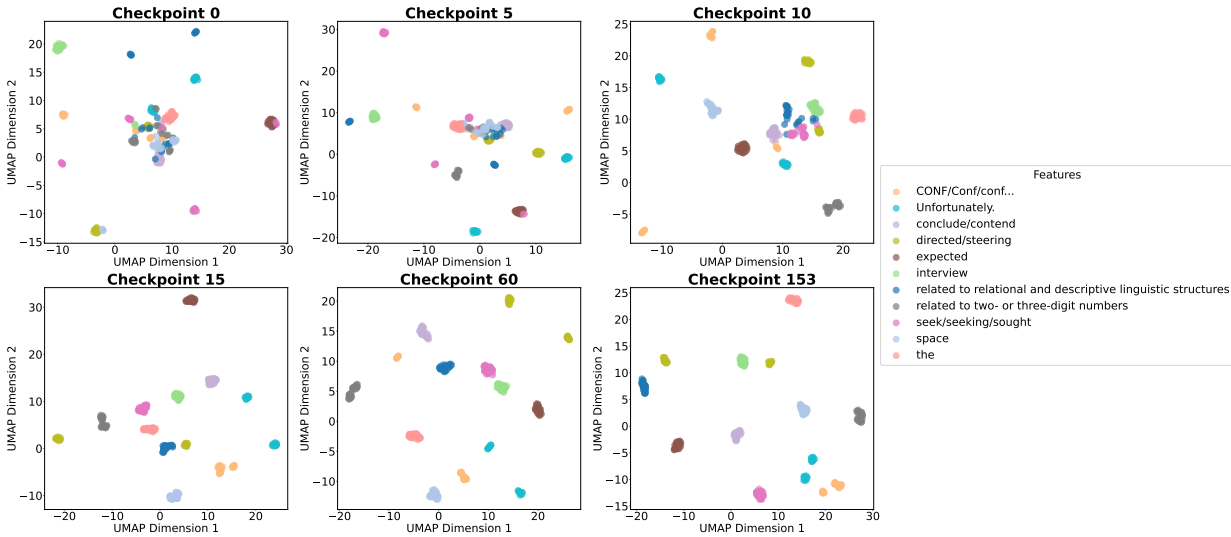


Figure 9. UMAP for Pythia-160m-deduped.

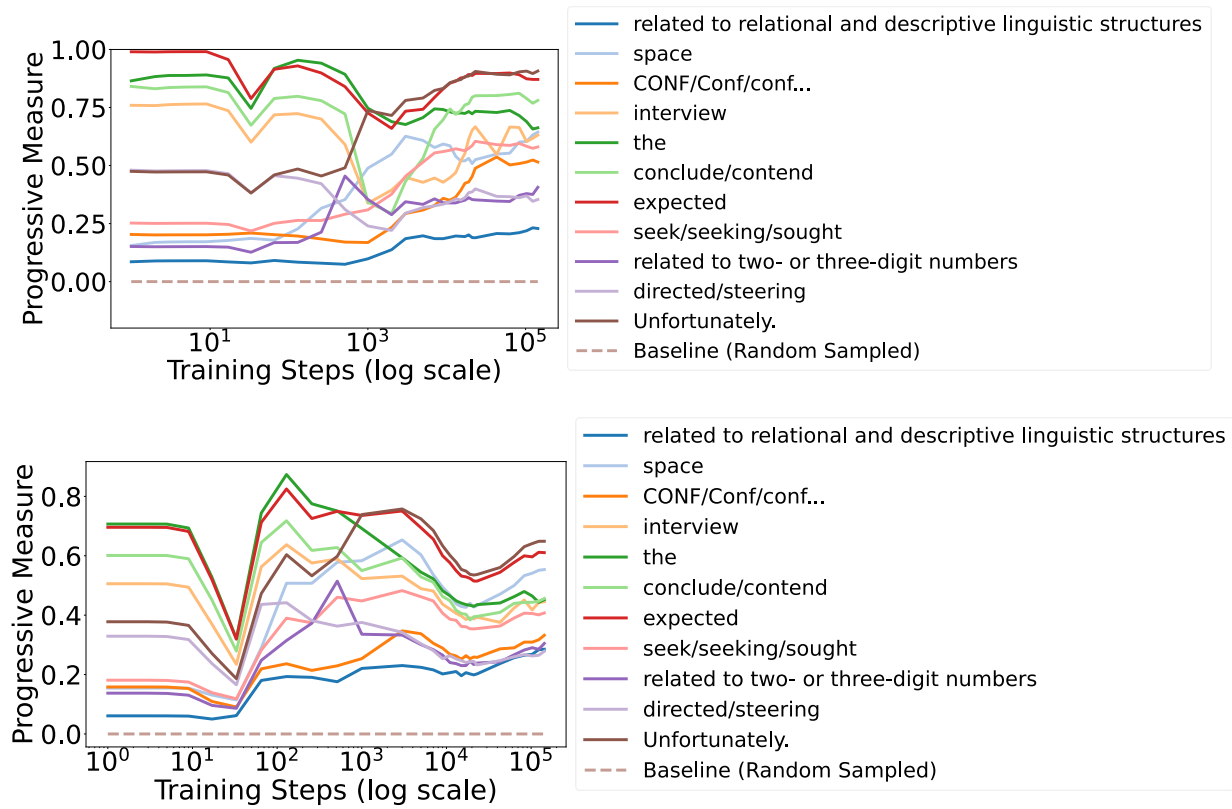


Figure 10. Progress Measure for Pythia-160m-deduped.

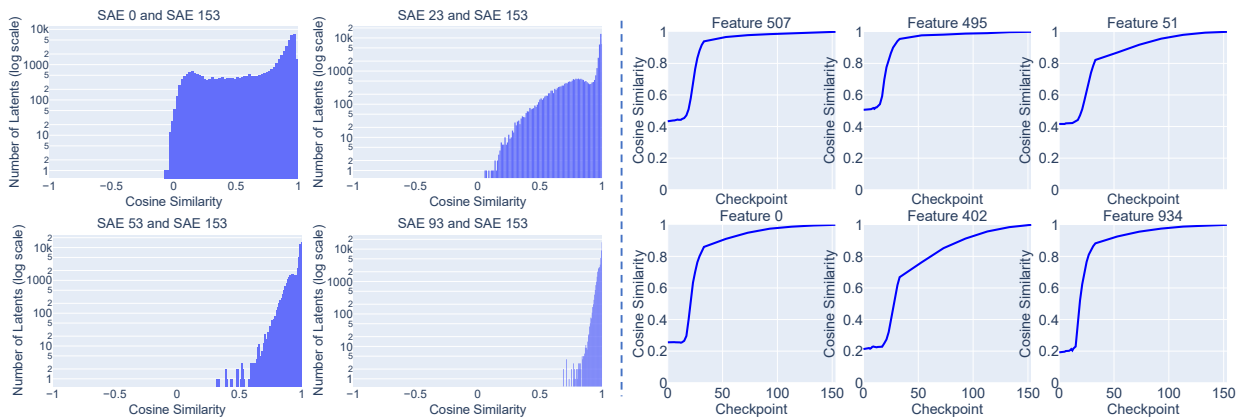


Figure 11. Cosine Similarity for Pythia-160m-deduped.

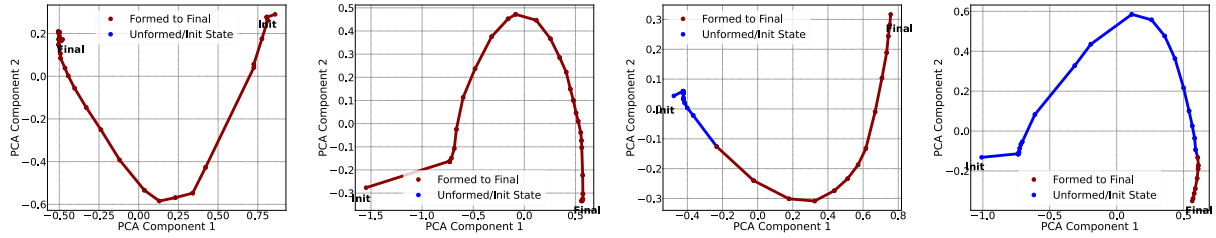


Figure 12. Feature Trajectories for Pythia-160m-deduped.

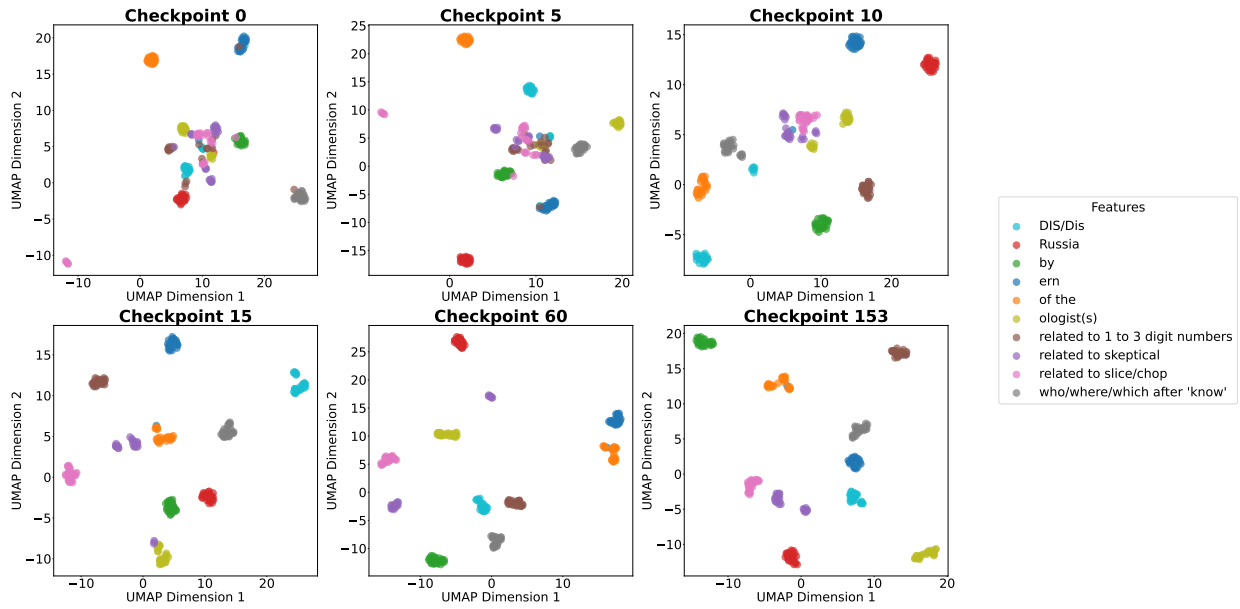


Figure 13. UMAP for Pythia-1.4b-deduped.

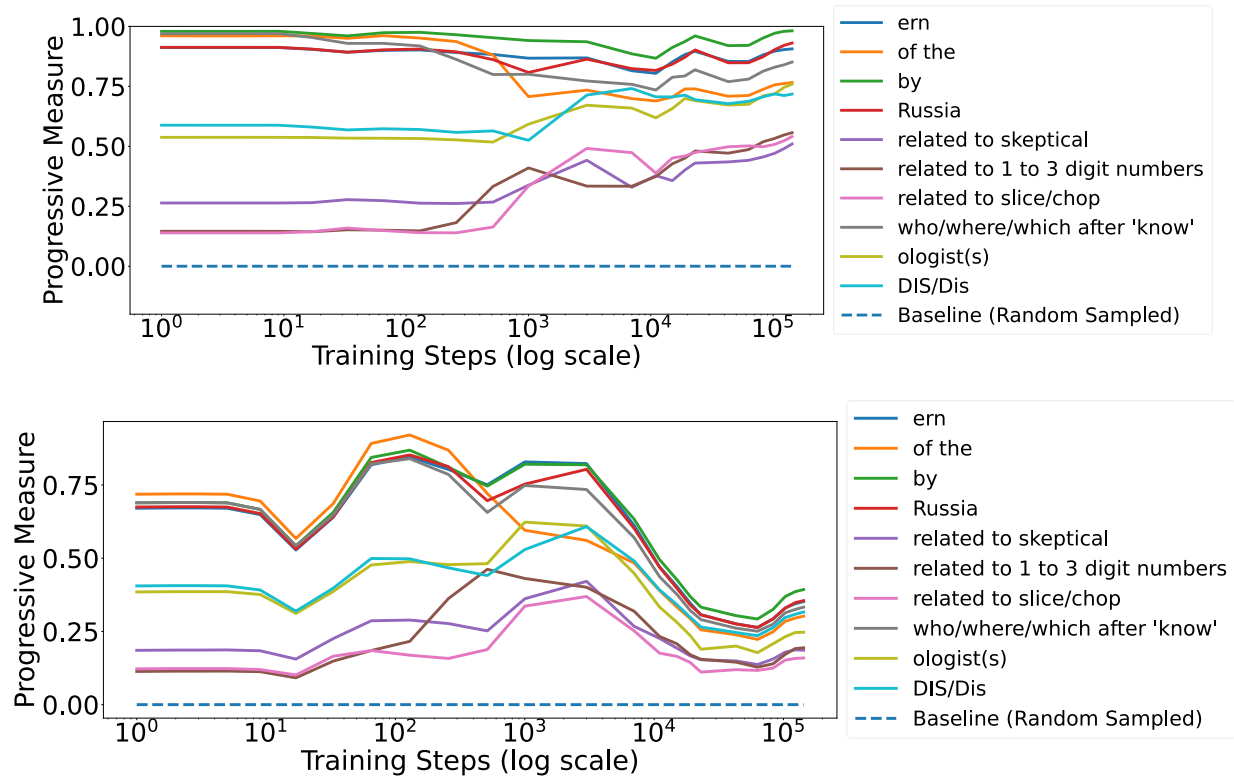


Figure 14. Progress Measure for Pythia-1.4b-deduped.

Tracking the Feature Dynamics in LLM Training: A Mechanistic Study

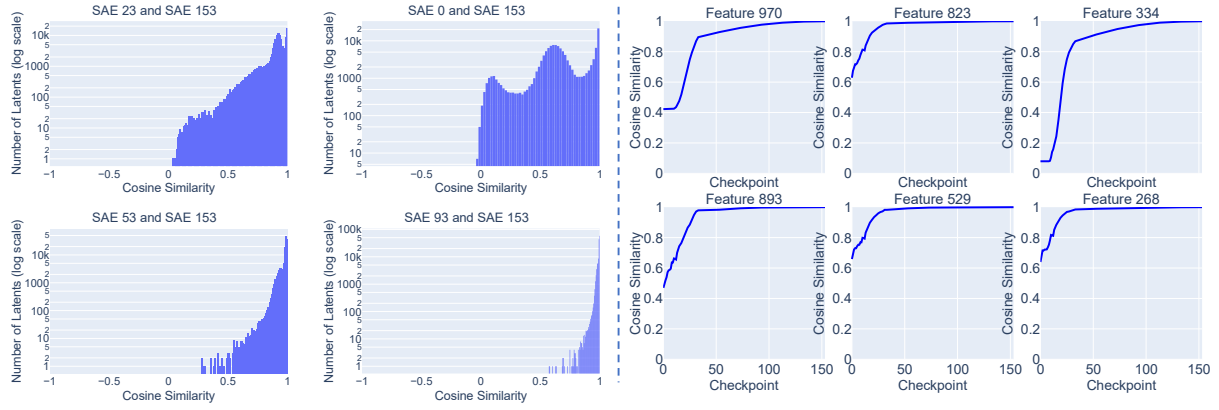


Figure 15. Cosine Similarity for Pythia-1.4b-deduped.

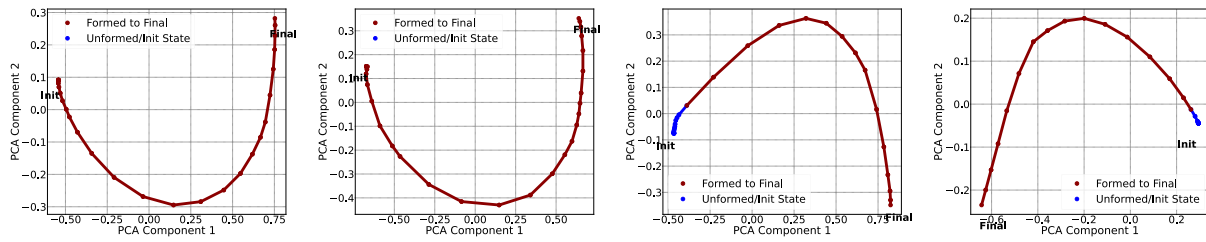


Figure 16. Feature Trajectories for Pythia-1.4b-deduped.

These results are consistent with those for **Pythia-410m-deduped** discussed in the main paper.